Original Article

Effect and mechanism of phospholipid scramblase 4 (PLSCR4) on lipopolysaccharide (LPS)-induced injury to human pulmonary microvascular endothelial cells

Xiaobin Liu, Dong Wang, Xiaoning Zhang, Meng Lv, Ge Liu, Changping Gu, Fan Yang, Yuelan Wang

Department of Anesthesiology and Perioperative Medicine, Shandong Qianfoshan Hospital, Cheeloo College of Medicine, Shandong University, Jinan, China

Contributions: (I) Conception and design: Y Wang, X Liu; (II) Administrative support: Y Wang; (III) Provision of study materials or patients: X Zhang, G Liu; (IV) Collection and assembly of data: M Lv; (V) Data analysis and interpretation: F Yang, D Wang; (VI) Manuscript writing: All authors; (VII) Final approval of manuscript: All authors.

Correspondence to: Yuelan Wang. Department of Anesthesiology and Perioperative Medicine, Shandong Qianfoshan Hospital, Cheeloo College of Medicine, Shandong University, No. 16766 Jingshi Road, Jinan 250014, China. Email: wyl0910@126.com.

Background: Previous experiments revealed phospholipid scramblase 4 (PLSCR4) mRNA to be significantly increased in a lipopolysaccharide (LPS)-induced acute respiratory distress syndrome (ARDS) model of human pulmonary microvascular endothelial cells (HPMECs); however, the effect of PLSCR4 and its mechanism have not been reported to date. The PLSCR family is thought to mediate the transmembrane movement of phospholipids (PS), and has been found to be involved in pyroptosis through combing with gasdermin D (GSDMD). We therefore speculated that PLSCR4 may contribute to cell death via pyroptosis.

Methods: To investigate the effect and mechanism of PLSCR4 in ARDS, we constructed an in vitro model of LPS-induced ARDS in HPMECs transfected with PLSCR4 small interfering RNA (siRNA) or scramble siRNA (sc siRNA). After 4 h of LPS stimulation, western blotting, immunoprecipitation, enzyme-linked immunosorbent assay (ELISA), tracer flux assays, and fluorescence assays were used to study the relationship between PLSCR4 and pyroptosis with regards to their impact on ARDS. We also established an ARDS mouse model which was pretreated with a liquid complex of PLSCR4 siRNA/sc siRNA-lipofectamine 2000 through the fundus venous plexus. Finally, we used DNA pull-down and protein profiling to study the potential transcription factor of PLSCR4.

Results: It was found that when the expression of PLSCR4 was elevated, the concentration of interleukin 1 beta (IL-1β) and IL-18 decreased, along with barrier damage ($P<0.05$). Furthermore, HPMEC injury was reduced with more distribution of PS and N-terminal cleavage product (GSDMD-NT) of GSDMD on the external side of cell membrane. However, the pyroptosis-relevant proteins of GSDMD and caspase-1 were not obviously changed ($P<0.05$); we further found that when PLSCR4 was depressed, the lung injury was aggravated in the mice. In the DNA pull-down assay, P62280 remarkably increased, which suggested that P62280 might be the transcription factor for PLSCR4.

Conclusions: PLSCR4 alleviated pyroptosis by transporting PS to the outside of the membrane, blocking the formation of pyroptosis pores composed of GSDMD. Moreover, P62280 might be the transcription factor of PLSCR4. These insults may provide useful insights into the clinical treatment of ARDS.

Keywords: Lipopolysaccharide (LPS); phospholipid scramblase 4 (PLSCR4); human pulmonary microvascular endothelial cells (HPMECs); pyroptosis; gasdermin D (GSDMD)

Submitted Dec 04, 2020. Accepted for publication Jan 08, 2021.
doi: 10.21037/atm-20-7983
View this article at: http://dx.doi.org/10.21037/atm-20-7983

Introduction

Acute respiratory distress syndrome (ARDS), featured by inflammatory injury, is one of the main causes of death in patients with multiple organ dysfunction caused by sepsis, and has a high morbidity and mortality rate (1,2).The main pathological characteristics of ARDS are the release of inflammatory factors, the infiltration and aggregation of inflammatory cells, and damage to the vascular endothelium that ultimately lead to changes in pulmonary microvascular endothelial permeability and pulmonary edema (3).

Despite the extensive research on ARDS, there are currently no effective drug treatments for this condition (1). In our previous study, high-throughput cell sequencing and bioinformatics analysis were conducted, showing the mRNA expression of phospholipid scramblase 4 (PLSCR4) protein to be significantly increased and centrally located in the co-expression network diagram (4,5). This suggested to us that PLSCR4 may play an important role in the injury of the human pulmonary microvascular endothelial cells induced by lipopolysaccharide (LPS) (*Figure 1*). However, the specific role and mechanism have not thus far been reported.

PLSCRs are a group of single pass, plasma membrane (PM) proteins that can mediate the nonspecific, bidirectional, and headgroup-independent transbilayer movement of phospholipids (PS) across the lipid bilayers, with PS being transported across the membrane in a Ca^{2+}-dependent manner, increasing its exposure on the cell membrane (6,7). The exofacical exposure of PS has been considered to be an important marker in mang Pathological processes like inflammatory responses and plays an important part in multiple cell types (8). In recent years, some studies have reported that in the process of inflammatory cell death-pyroptosis, the function of the pyroptosis executive protein, gasdermin D (GSDMD) may have a significant relationship with PS (9). Therefore, this study aimed to explore the biological effect and mechanism of PLSCR4 in the process of acute pulmonary microvascular endothelial injury caused by LPS, and its relationship with pyroptosis. We present the following article in accordance with the ARRIVE reporting checklist (available at http://dx.doi.org/10.21037/atm-20-7983).

Methods

Kits, antibodies, and reagents

PLSCR4 siRNA was synthesized and supplied by GenePharma (Shanghai, China). The PLSCR4 antibody was purchased from Abcam (Cambridge, UK). GSDMD, caspase-1 and caspase-1 P20 antibodies were purchased from Cell Signaling Technology (Danvers, MA, USA). The interleukin 1 beta (IL-1β) and IL-18 enzyme-linked immunosorbent assay (ELISA) detection kits were provided by Elabscience Biotechnology Co., Ltd. (Wuhan, China). The annexin V-FITC cell pyroptosis detection kit was purchased from Beyotime Biotechnology (China). The Transwell filter insert for tracer flux assays was purchased from Corning Inc. (Corning 3401, 12-mm diameter, 0.4-μm pore size; Corning, NY, USA). The fluorescein isothiocyanate (FITC)-dextran was purchased from Sigma-Aldrich (St. Louis, MO, USA).

Cell culture

The HPMECs were purchased from ScienCell Research Laboratories (Carlsbad, CA, USA). The cell recovery, culture, and subculture were carried out in a cell incubator at 37 ℃ with 5% CO_2, according to the standard operating instructions provided by ScienCell Research Laboratories (Carlsbad, CA, USA). In our study, the cell culture medium, serum, growth factor, and antibiotics used were all recommended by ScienCell. HPMECs were divided into 4 groups: sc siRNA, sc siRNA + LPS, PLSCR4 siRNA + LPS, and PLSCR4 siRNA group.When the culture reached 80–90% confluency, LPS was added to the working solution in the wells of experimental groups to reach a final concentration of 1 μg/mL, and cultured for 4 h.

Small interfering RNA (siRNA)-mediated knockdown

Cells were seeded in a 6-well plate the day before the transfection, and cell growth was observed the following day. When the confluency reached 50–70%, the HPMECs could be transfected. A nuclease-free Eppendorf (EP) tube was prepared in advance. Then, 200 μL of the basic medium was added to the EP tube, and 5.5 μL of 20 μM of siRNA (5' to 3' sequence was GGAAGUGGAAUGGUUUGUUTT) was added. After being mixed up and down by a pipette, 16 μL of transfection reagent INTERFERin (Polyplus-transfection, New York, NY, USA) was added and incubated at room temperature for 10 min. Then, the culture medium was changed during incubation, the 6-well plate was rinsed twice with sterile Dulbecco's Phosphate Buffered Saline (DPBS) solution, and 2 mL of fresh complete medium was added. After incubation, the transfection complex was added

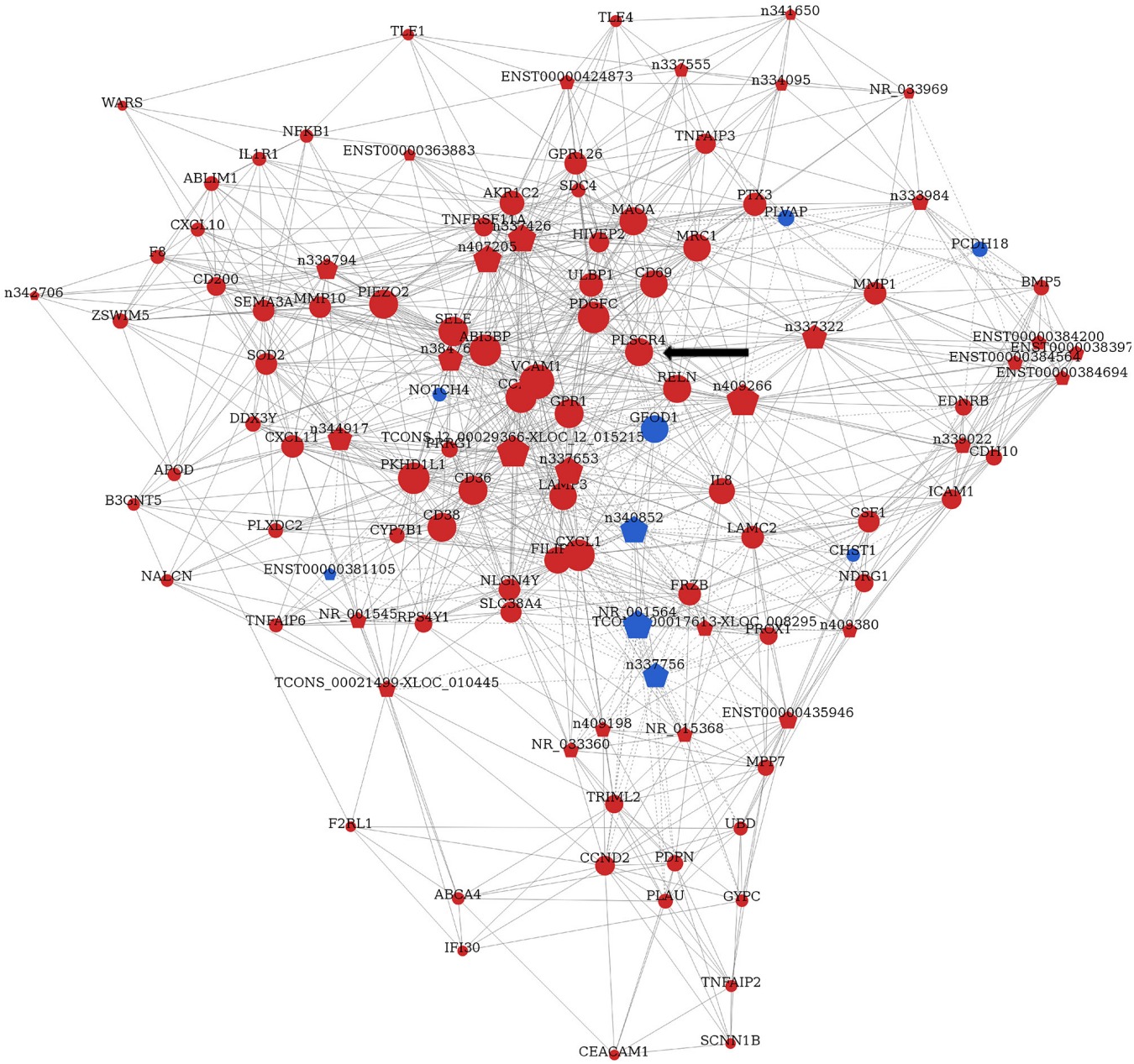

Figure 1 Co-expression network of differentially expressed mRNAs and interacting expression of lncRNAs in HPMECs exposed to LPS. The pentagons represent lncRNAs, and the circles represent mRNAs. Blue dots and red dots indicate downregulated and upregulated RNAs respectively, with the size representing the degree of upregulation and downregulation. The arrow indicates the expression of PLSCR4. HPMEC, human pulmonary microvascular endothelial cell; LPS, lipopolysaccharide; PLSCR4, phospholipid scramblase 4.

to the 6-well plate. The concentration of the siRNA was 50 nM. After being mixed, these cells were incubated at 37 ℃ for 2 days, and their protein expression was then analyzed.

Animals

Eighty wild-type male C57BL/6 mice (8–10 weeks, 20–25 g) from Vital River Laboratory (Beijing, China) were randomly divided into 4 groups and housed under specific pathogen-free conditions. The experiments were approved by the Animal Ethics Committee of Qianfoshan Hospital of Shandong University (No.: 2019-016). A liquid complex of PLSCR4 siRNA/scramble siRNA (sc siRNA)-Lipofectamine 2000 was injected through the fundus venous plexus twice a week in a solution of 150 μL PLSCR4 siRNA/sc siRNA (40 μM) (GenePharma, China) with 16 μL of Lipofectamine 2000 diluted in 100 μL diethyl pyrocarbonate (DEPC)-treated water. After anesthesia, the mice in the experimental group were injected with LPS (6 mg/kg) through the trachea via tracheotomy. Then, the mice were placed upright and rotated vertically to ensure the drug was evenly distributed in the alveolus After 24 h of tracheal instillation, the mice were sacrificed, and the lung tissue was collected for further pathological examination. Experiments were performed in compliance with the guidelines of Animal Ethics Committee of Qianfoshan Hospital of Shandong University for the care and use of animals.

Extraction of protein and Western blotting

For total protein extraction, 100 μL of cell lysate containing radio immunoprecipitation assay (RIPA) and phenylmethanesulfonyl fluoride (PMSF) (RIPA:PMSF =100:1) was added in each well of the 6-well plate, and the plate was set on ice for 30 min. After the lysis, the cell lysate was collected in a 1.5-mL EP tube. Subsequently, the centrifuge processing of the lysate was carried out at 12,000 rpm for 15 min at 4 ℃. After centrifugation, the supernatant was transferred to another EP tube to obtain the total protein. The total protein concentration was detected using a bicinchoninic acid (BCA) protein estimation kit, and 5× loading buffer was added to the protein samples, which was then heated and denatured at 96 ℃ for 5 min. The protein of the membrane and cytoplasm that aimed to test the distribution of GSDMD-NT was extracted according the instructions of the protein extraction kits. Cell were centrifugated at 4 ℃, at 500 g for 3 min, and then washed twice with cold PBS; then, 200 μL of cold reagent A, 2 μL of protease inhibitor mixture, and 2 μL of protein stabilizer were added, and followed by high-speed vortex oscillation for 5 sec and centrifugated at 4 ℃ with 13,000 g for 5 min. The supernatant was transferred to another EP tube, subjected to a 37 ℃ water bath for 10 min, and then centrifuged at 37 ℃ for 5 min; the upper solution was considered the cytoplasmic protein, while the lower solution was diluted with reagent B and C in turn, and was considered the membrane protein.

The obtained protein samples were subjected to SDS-PAGE (sodium dodecyl sulfate-polyacrylamide gel electrophoresis) gel electrophoresis, and transferred onto polyvinylidene fluoride (PVDF) membranes. The membranes were then blocked with 5% skimmed milk for 1 h at room temperature, and the sample was washed with tris-buffered saline with Tween20 (TBST) for 5 min 3 times at the end of blocking. The membranes were incubated in the primary antibody diluent (1:1,000) overnight at 4 ℃. The next day, the membranes were incubated in the secondary antibody diluent (1:5,000) at room temperature for 1 h, and finally set on the scan machine (10).

ELISA detection of IL-1β and IL-18

After 4 h of stimulation by LPS, the supernatant of each group of cells in the 6-well plate was collected and added to an EP tube. The supernatant was centrifuged at 1,000 g for 20 min at 4 ℃ to remove the impurities and cell debris. The double-antibody sandwich ELISA kit was used for the detection of inflammatory factors IL-1β and IL-18 (11), which were used to assess the pyroptosis. If these could not be detected in time, the sample was frozen at –80 ℃ to avoid repeated freezing and thawing.

Tracer flux assays

In this study, tracer flux assays were performed to detect the changes in endothelial permeability. The Transwell chamber (Corning Inc.) had a filter pore diameter of 0.4 μm and a cell diameter of 12 mm. Next, 1.5 mL of complete medium was added to the bottom chamber, and 0.5 mL of complete culture medium that contained the suspended cells was added to the upper chamber. The number of HPMECs was 5×10^5. Afterwards, the Transwell chamber was cultured in an incubator at 37 ℃. The next day, the medium was changed, and the cell adhesion was

observed under a microscope. After 1–3 days, when the cell confluency reached 90%, the medium in the bottom layer for the experimental group was replaced with fresh medium containing 1 μg/mL of LPS, while the medium in the upper chamber was replaced with fresh culture containing 1 μg/mL of LPS and 1 mg/mL of FITC-dextran. The upper and lower layers of the chamber for the blank control group did not contain LPS, and the upper layer only contained 1 mg/mL of FITC-dextran. Both groups were placed in a cell incubator at 37 ℃ to continue culturing for 4 h. After 4 h, 50 μL of the bottom culture medium of each group was taken and added to a 96-well plate. After labeling, the samples were placed in a fluorescence microplate reader (BioTek Synergy H1m, Agilent, USA) to read the data. The excitation light wavelength of the microplate reader was set to 488 nm, and the emission wavelength was set to 520 nm (12). Data analysis was expressed by permeability index (PI), which is the ratio of the fluorescence intensity of each experimental group to the wells without cells.

Pyroptosis fluorescence assays

Fluorescence experiments were performed to detect the degree of pyroptosis of HPMECs (13). The endothelial cells were seeded in a 24-well plate. The medium was changed with 1 mL of fresh and complete culture on the next day, and then cultured for 1–2 days. When the cell confluency reached 80–90%, LPS (1 μg/mL) was added to the experimental group, and the HPMECs were cultured for 4 h. After the stimulation, cells in each group were washed twice with DPBS. Next, 96 μL of Annexin V-FITC binding solution, 1 μL of Annexin V-FITC (green fluorescence), and 12.5 μL of PI (propidium iodide,red fluorescence) were added to each well. After mixing, the samples were placed on ice and placed in the dark for 10 min. Finally, an immunofluorescence microscope (Leica DMi8, Leica Microsystems, Wetzlar, Germany) was used to observe the endothelial cell membrane staining. The Annexin V-FITC fluorescence intensity reflected the degree of PS exposure on the cell membrane surface. The PI fluorescence intensity represented the degree of cell membrane integrity damage.

Lung injury scores, wet/dry weight ratio, hematoxylin-eosin (HE) staining

To describe the pathological changes among groups, the lung injury score was evaluated based on edema, hyaline membrane formation, thickened alveolar septa, alveolar hemorrhage, destroyed pulmonary architecture, and infiltration of inflammatory cells. The score ranged from 0 to 4, respectively representing no damage, mild damage, moderate damage, severe damage, and very serious damage.

The wet/dry ratio of the lung is not only a direct indicator of pulmonary edema, but also a sensitive index to reflect the severity of lung injury. After each group of mice was sacrificed, the whole lung was taken out, and the wet weight was weighed. Then the lung tissue was dried in a 65 ℃ incubator. After 24 h, the dry weight was taken out to calculate the wet/dry ratio of the lung.

The right lung was fixed with 4% paraformaldehyde, then dehydrated, embedded in paraffin, and sectioned (5 μm). The HE-stained sections were observed under a light microscope at a magnification of 400×.

DNA pull-down and protein profiling

In order to determine the possible transcription factors of PLSCR4, our study used the DNA pull-down and protein profiling techniques. T-75 flasks were used to cultivate HPMEC cells. These were divided into a control group (ctrl group) and an experimental group (exp group), with each group having more than 2×10^7 cells. The PLSCR4 promoter sequence probe was synthesized and labeled according to the National Center for Biotechnology Information Company (NCBI) gene library information, and two sets of cellular proteins were extracted for the DNA pull-down. After the coupling biotin probe bonded with the magnetic beads that were coupled to streptomycin, the probe reacted with the sample, and the protein that was bound to the probe was obtained. After one-dimensional or two-dimensional electrophoresis, the gel strips and dots of the target protein were obtained, and the in-gel enzymatic hydrolysis method was optimized. If there was a clear difference between the exp group and ctrl group, mass spectrometry was performed. In this study, liquid chromatography-tandem mass spectrometry (LC-MS/MS) technology was used to analyze and obtain relevant information, including the charge and peak map of the protein fragmentation fragments. Proteinpilot database software (SCIEX, Framingham, MA, USA) was used to perform bioinformatics analysis on the obtained results. The mass spectrometry analysis results and the silver staining results were analyzed together to obtain the protein information of the target gel point, or the potential transcription factor of PLSCR4.

Statistical analysis

Each group of experiments was repeated at least 3 times. The experimental data are expressed as mean ± standard deviation. One-way ANOVA was used for comparisons between groups. All data were analyzed and processed using the SPSS 22.0 statistical software (IBM Corp., Armonk, NY, USA). A P value <0.05 indicated that the difference was statistically significant.

Results

PLSCR4 mRNA significantly increased in LPS-induced HPMECs

In our preliminary work, in order to find the remarkably changed mRNA in ARDS, we used LPS to stimulate HPMECs for 4 h. Then we performed microarray analysis of RNA expression by using Affymetrix Human Transcriptome Array 2.0. We found that 183 mRNA increased, and 29 mRNA decreased. Amony which, PLSCR4 mRNA was one of the most remarkably increased mRNA and centrally located in the co-expression diagram (*Figure 1*).

PLSCR4 was closely correlated to the pyroptosis and permeability of the HPMECs

In recent years, research on cell death methods has revealed a new type of programmed and inflammatory cell death pyroptosis (14). The characteristic pathological changes of cell pyroptosis are accompanied by secretion of IL-1β and IL-18 release (15,16), and damage to the integrity of the cell membrane. Hence, cell pyroptosis is also called cell inflammatory necrosis (17,18). In order to verify the change of PLSCR4 expression in vascular endothelial cells and its correlation with the degree of pyroptosis and permeability change, HPMECs were divided into 4 groups: sc siRNA, sc siRNA + LPS, PLSCR4 siRNA + LPS, and PLSCR4 siRNA group.

It was found that the expression level of PLSCR4 in the sc siRNA + LPS group significantly increased compared to the sc siRNA group, which is consistent with the previous high-throughput sequencing results (*Figure 2A*). After PLSCR4 siRNA silencing, the expression level of PLSCR4 decreased markedly in the PLSCR4 siRNA + LPS group compared with the sc siRNA + LPS group. The ELISA results revealed that after LPS stimulation, the concentration of IL-1β and IL-18 in the cell culture medium of group sc siRNA + LPS significantly increased compared to the sc siRNA group. Furthermore, the increase in PLSCR4 in the siRNA + LPS group was greater (*Figure 2B,C*), suggesting that PLSCR4 may have the effect of reducing the release of IL-1β and IL-18 from HPMECs. The tracer flux assay results revealed the same trend among the 4 groups (*Figure 2D*). These results indicated that with the decrease of PLSCR4 expression, the degree of inflammatory response of pyroptosis in HPMECs after the LPS stimulation and the permeability of endothelium increased. This suggests that PLSCR4 may play an important anti-inflammatory role in pyroptosis and in maintaining endothelial permeability.

PLSCR4 alleviated pyroptosis through PS, but had no effect on the proteins of the pyroptosis pathway

In order to verify the mechanism of PLSCR4 upon pyroptosis, fluorescence assays and western blotting were performed.

Compared with the sc siRNA + LPS group, the green fluorescence of Annexin V-FITC on the HPMECs surface of the PLSCR4 siRNA + LPS group was decreased, while the red fluorescence of PI was increased (*Figure 3A*). However, there was no obvious change in the sc siRNA group and PLSCR4 siRNA group. This suggests that when the expression of PLSCR4 was too low to transport PS outside of the cell membrane, the destruction of the cell membrane of the HPMECs increased; furthermore, N-GSDMD might form more transmembrane pores, which was also consistent with the increase in the concentration of IL-1β and IL-18 in the cell culture medium. The western blotting results revealed that when the expression level of PLSCR4 changed, the expression of pyroptosis-related proteins were not affected (*Figure 3B*), but the distribution of N-GSDMD increased significantly in the PLSCR4 siRNA group, compared with the sc siRNA + LPS group (*Figure 3C*). Hence, it was presumed that PLSCR4 could reduce the pyroptosis of HPMECs by transferring PS outside of the cell membrane, with no significant effect on the proteins of the pyroptosis.

The role of PLSCR4 in LPS-induced lung injury

C57BL/6 mice were used to determine the role of PLSCR4 in the ARDS model. As shown in *Figure 4A,B,C*, mice in the PLSCR4 siRNA group received higher scores than mice in the sc siRNA group. To observe the lung injury directly,

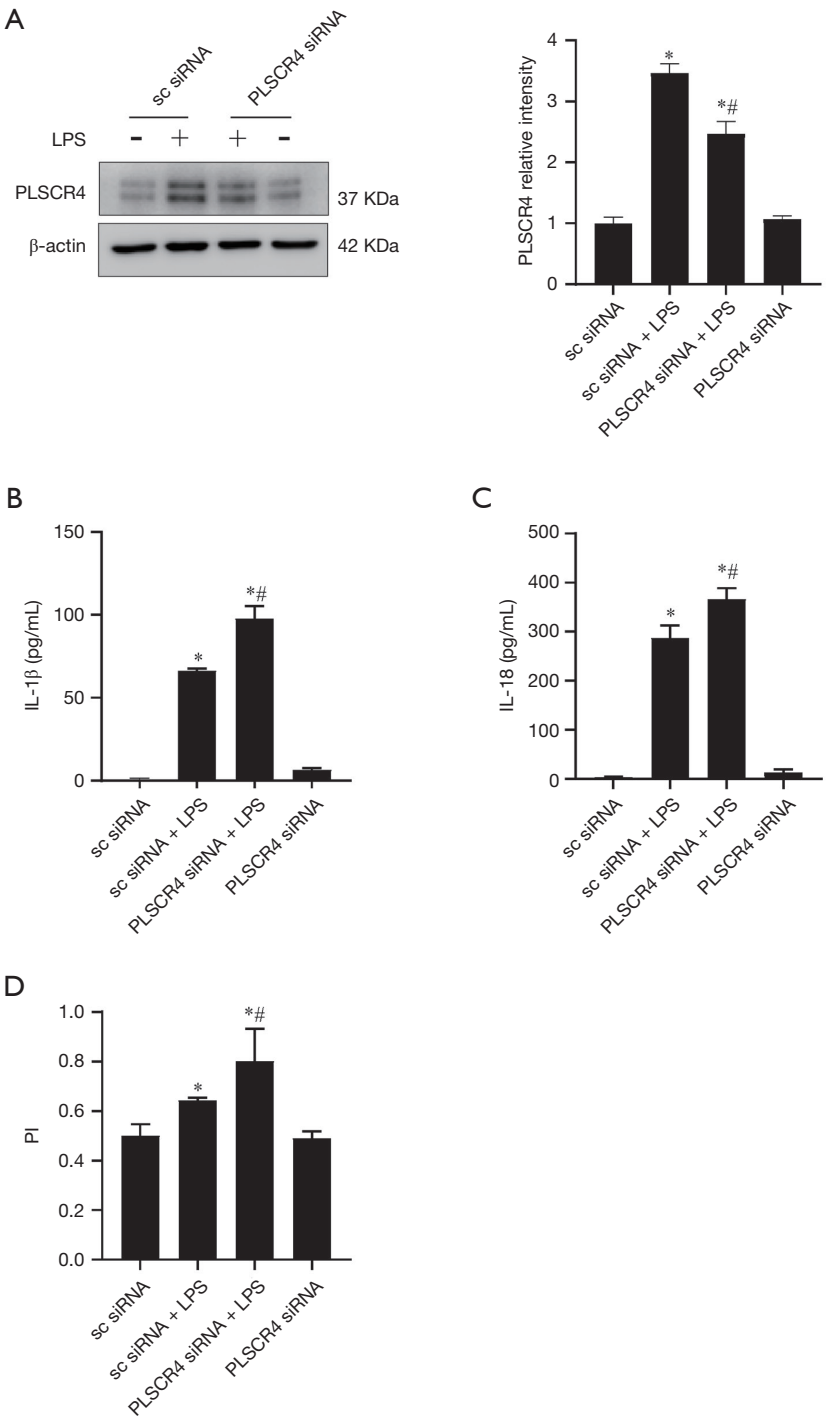

Figure 2 PLSCR4 was closely correlated to the pyroptosis and permeability changes of HPMECs. (A) The expression level of PLSCR4 significantly increased after LPS stimulation and decreased after siRNA silencing. (B,C) After PLSCR4 siRNA silencing, the concentration of IL-1β and IL-18 in the cell culture medium significantly increased in PLSCR4 siRNA + LPS group. (D) After silencing the PLSCR4, the increase in HPMEC permeability in PLSCR4 siRNA + LPS group during LPS stimulation was more significant than that in the sc siRNA + LPS group. *P<0.001 *vs.* the sc siRNA group; #P<0.05 *vs.* the sc siRNA + LPS group. PLSCR4, phospholipid scramblase 4; HPMEC, human pulmonary microvascular endothelial cell; LPS, lipopolysaccharide; siRNA, small interfering RNA; sc siRNA, scramble siRNA.

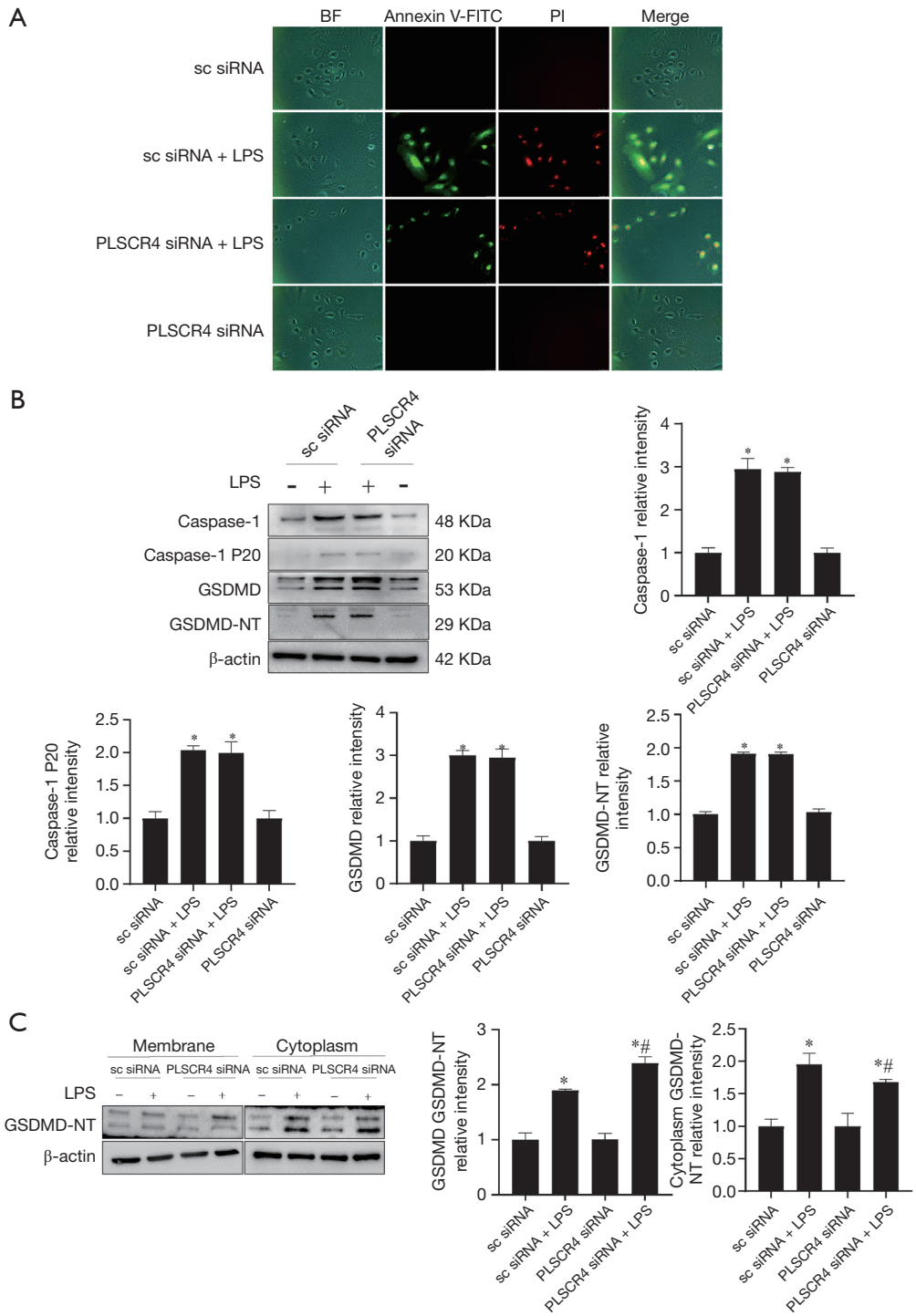

Figure 3 PLSCR4 affected cell pyrolysis through PS, but had no effect on the related protein activity of the pyrolysis pathway. (A) After inhibiting the expression of PLSCR4, there was less PS outside the cell membrane. Furthermore, the integrity of the cell membrane was destroyed, and the PI staining of the nucleus was enhanced (magnification 200×). (B) The change in expression of PLSCR4 had no significant effect on the pyrolysis-related proteins during cell pyrolysis. (C) After the depletion of PLSCR4, more GSDMD-NT was distributed on the membrane of HPMECs and less distributed in the cytoplasm when HPMECs was stimulated by LPS. *P<0.001 *vs.* the sc siRNA group; #P<0.05 *vs.* the sc siRNA + LPS group. PLSCR4, phospholipid scramblase 4; PS, phospholipids; GSDMD, gasdermin D; siRNA, small interfering RNA; sc siRNA, scramble siRNA.

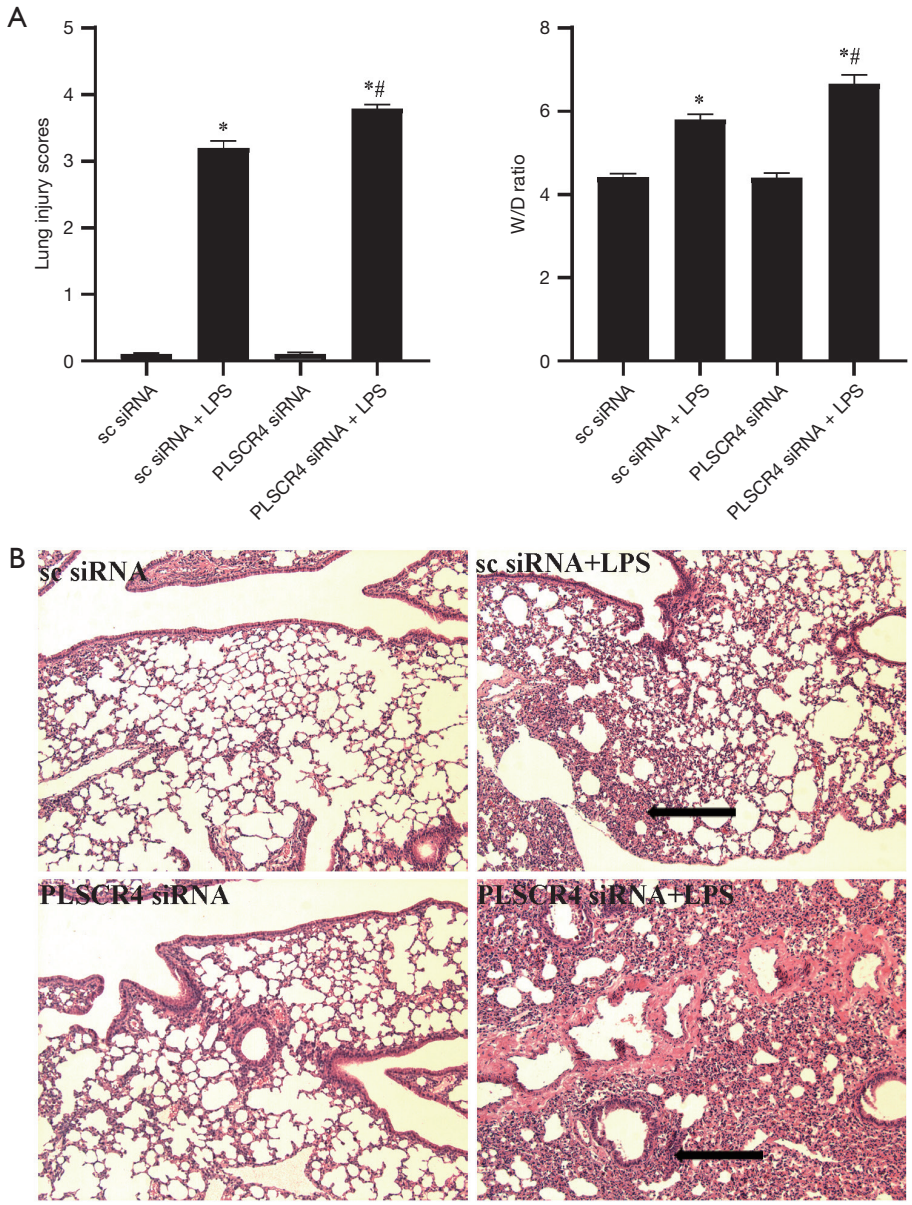

Figure 4 Effect of PLSCR4 on LPS-induced lung injury. (A) Lung injury scores were used to evaluate the severity of lung injury in different groups. (B) The degree of pulmonary edema was evaluated by wet/dry ratio. (C) The pathological changes of mice lung tissues were assessed by HE staining (magnification 400×). *P<0.001 *vs.* the sc siRNA group; #P<0.05 *vs.* the sc siRNA + LPS group. PLSCR4, phospholipid scramblase 4; LPS, lipopolysaccharide; HE, hematoxylin-eosin; siRNA, small interfering RNA; sc siRNA, scramble siRNA.

HE staining was used to assess pathological changes. As shown in *Figure 4C*, the destruction of pulmonary architecture, interstitial edema, alveolar hemorrhage, and infiltration of inflammatory cells was obviously apparent in the sc siRNA + LPS group, and was even worse in the PLSCR4 siRNA + LPS group, which was consistent with the scores above.

The wet/dry ratio was used to assess the pulmonary edema. As shown in *Figure 4B*, the wet/dry ratio had a greater increase in the PLSCR4 siRNA + LPS group than in the sc siRNA + LPS group, which indicated that the depletion of PLSCR4 aggravated the pulmonary edema.

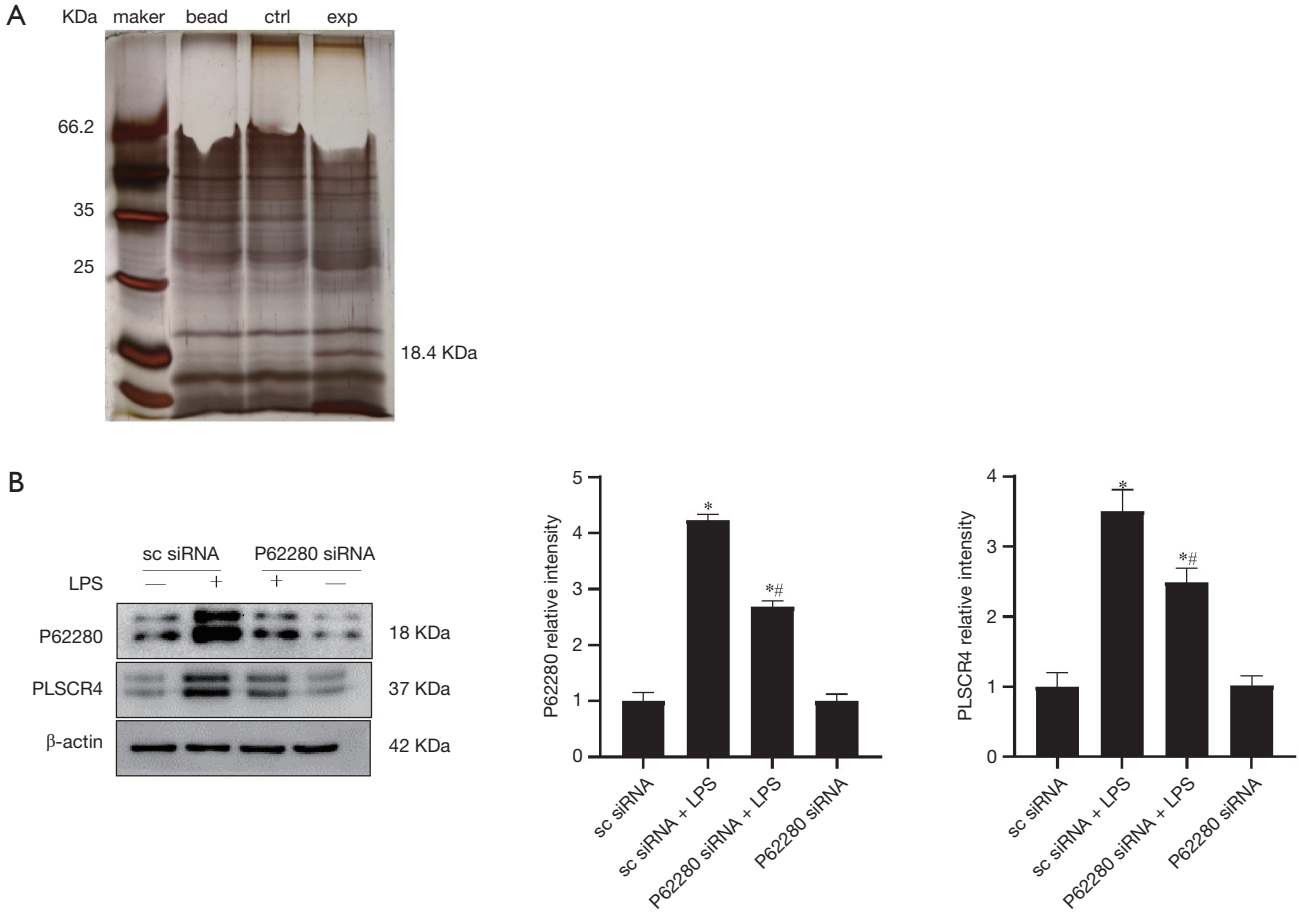

Figure 5 P62280 might regulate the expression of PLSCR4 as a transcription factor. (A)The SDS-PAGE silver staining results for the two groups of protein samples after DNA pull-down. The ctrl group is a blank control group. The exp group is the experimental group. The bead group is the blank magnetic bead control group without the DNA probe. The results revealed that at a molecular weight of 18.4 KDa, the exp group was significantly different from the other groups. (B) After silencing P62280, the expression level of PLSCR4 decreased. *P<0.001 *vs.* the sc siRNA group; #P<0.05 *vs.* the sc siRNA + LPS group. PLSCR4, phospholipid scramblase 4; siRNA, small interfering RNA; sc siRNA, scramble siRNA.

DNA pull-down and protein profiling for examining PLSCR4 transcription factor

In order to further the understanding of the upstream mechanism of PLSCR4, our study explored the upstream transcription factor of PLSCR4 using DNA pull-down and protein profiling technology.

The silver staining results for the control group and experimental group revealed that there was a significant difference between these two groups at the 18.4 KDa molecular weight (*Figure 5A*). In the protein profiling experiment, when the reliability was set to a confluence of ≥95% and unique peptides ≥1, the number of secondary spectra generated by the sample mass spectrometer were 6,830 and 2,765 respectively, and the number of resolved secondary spectra were 1,685 and 423, respectively. Common contaminated proteins and matching peptides were filtered out. The overall situation of the proteins identified by the sample from the ctrl group are presented in *Table 1*, and the information of the proteins from the exp group are presented in *Table 2*. The molecular weight of 18.4 KDa was obtained and identified as P62280 (*Table 2*).

In order to verify the results of the DNA pull-down and protein profiling, and to determine whether P62280 can be used as an upstream transcription factor to exert endothelial protection by regulating the expression of PLSCR4,

Table 1 Information of the top 20 proteins identified by the sample from the control group

Accession	Length	Mass (Da)	Unused	Coverage (%)	Spectrum	Unique spectrum
sp|E9PAV3|NACAM_HUMAN	2,078	205,419	4.01	1.396	6	6
sp|P48047|ATPO_HUMAN	213	23,277.1	6.01	16.429999	4	4
sp|P17655|CAN2_HUMAN	700	79,994.5	1.47	3.4290001	3	3
sp|P62910|RL32_HUMAN	135	15,859.7	2	9.6299998	1	1
sp|P17987|TCPA_HUMAN	556	60,342.9	2.86	3.7769999	2	2
sp|Q15366|PCBP2_HUMAN	365	38,579.7	2	3.836	2	2
sp|O14776|TCRG1_HUMAN	1,098	123,900.1	7.34	2.9139999	4	4
sp|Q9Y2W2|WBP11_HUMAN	641	69,997	2	1.716	1	1
sp|Q92522|H1X_HUMAN	213	22,487	2	4.6950001	1	1
sp|P42766|RL35_HUMAN	123	14,551.4	4	11.38	2	2
sp|P15924|DESP_HUMAN	2,871	331,771.2	4.82	0.5225	2	2
sp|P04275|VWF_HUMAN	2,813	309,261.8	6.24	1.209	4	4
sp|Q9BTM1|H2AJ_HUMAN	129	14,019.3	2	20.93	13	3
sp|P23528|COF1_HUMAN	166	18,502.3	3.15	13.249999	6	6
sp|Q00341|VIGLN_HUMAN	1,268	141,454.5	4.09	2.366	3	3
sp|P27635|RL10_HUMAN	214	24,603.7	2.62	5.607	1	1
sp|P25398|RS12_HUMAN	132	14,514.8	2.15	6.8180002	2	2
sp|P10809|CH60_HUMAN	573	61,054.2	2	2.094	2	2
sp|P09661|RU2A_HUMAN	255	28,415.3	3.37	5.8820002	2	2
sp|Q12797|ASPH_HUMAN	758	85,862.1	3.16	2.2430001	3	3

Unused: protein identification score; Coverage: confluence ≥95% protein coverage; Spectrum: total spectrum amount; Unique Spectrum: unique spectrum amount.

HPMECs were divided into 4 groups: the sc siRNA group, the sc siRNA + LPS group, the P62280 siRNA + LPS group, and the P62280 siRNA group. The P62280 siRNA sequence (5' to 3') was CCAAACGACTTGGACGATGTT, and the antibody of P62280 was purchased from Abcam. Western blotting was used to detect the expression of PLSCR4 and the pyroptosis-related proteins.

After silencing P62280 by siRNA transfection, LPS continuously stimulated the HPMECs for 4 h. It was found that the expression of PLSCR4 was consistent with the change in P62280 (*Figure 5B*), suggesting that P62280 can regulate the expression level of PLSCR4 as a transcription factor.

Discussion

Acute lung injury or ARDS caused by sepsis appears as diffuse lung inflammation and pulmonary interstitial edema. The key step in this process is the microvascular barrier dysfunction caused by lung microvascular endothelial cell injury (19,20). In the past, investigations into the mechanism of sepsis-induced pulmonary microvascular endothelial cell damage mainly focused on endothelial cell death, and the processes of necrosis, apoptosis, and cytoskeletal remodeling (21,22). However, the exact mechanism remains unclear. In our preliminary experiments (4,5), high-throughput sequencing revealed that the PLSCR4 mRNA expression significantly increased after LPS stimulated HPMECs for 4 h. However, the specific role and mechanism of PLSCR4 have not yet been reported.

PLSCRs are a class of single-pass transmembrane proteins that can transfer PS from the inside to the outside of the cell membrane in a Ca^{2+}-dependent

Table 2 Information of proteins from the experimental group treated with LPS

Accession	Length	Mass (Da)	Unused	Coverage (%)	Spectrum	Unique spectrum
sp|Q7L7L0|H2A3_HUMAN	130	14,121.4	2.52	6.9229998	9	9
*sp|P62280|RS11_HUMAN	158	18,430.6	3.54	8.8610001	2	2
sp|Q00325|MPCP_HUMAN	362	40,094.5	6	8.0109999	3	3
sp|P07305|H10_HUMAN	194	20,862.8	1.66	4.6390001	1	1
sp|Q9Y324|FCF1_HUMAN	198	23,369.4	2	5.556	1	1
sp|P63261|ACTG_HUMAN	375	41,792.5	20.46	19.73	12	12
sp|P12236|ADT3_HUMAN	298	32,866	5.82	8.3889998	5	5
sp|P20073|ANXA7_HUMAN	488	52,738.9	2	2.2539999	1	1
sp|P0DPH8|TBA3D_HUMAN	450	49,959.1	8.47	7.9999998	6	6
sp|P06899|H2B1J_HUMAN	126	13,904.1	2.18	47.620001	16	1
sp|Q9HD33|RM47_HUMAN	250	29,450.1	1.33	3.2000002	1	1
sp|Q2VIR3|IF2GL_HUMAN	472	51,228.2	3.01	4.4489998	2	2
sp|P05121|PAI1_HUMAN	402	45,059.7	2.84	1.7410001	1	1
sp|O60814|H2B1K_HUMAN	126	13,890	13.78	47.620001	17	2
sp|Q9H0S4|DDX47_HUMAN	455	50,646.1	2	1.7580001	1	1
sp|O00422|SAP18_HUMAN	153	17,561	1.81	5.229	1	1
sp|P18206|VINC_HUMAN	1,134	123,798.1	4.19	2.028	2	2
sp|P05362|ICAM1_HUMAN	532	57,824.8	2	1.692	1	1
sp|P05388|RLA0_HUMAN	317	34,273.2	4.67	7.2559997	4	4
sp|Q96GQ7|DDX27_HUMAN	796	89,834.5	2	1.382	1	1
sp|P06703|S10A6_HUMAN	90	10,179.6	2	8.8890001	1	1
sp|Q14444|CAPR1_HUMAN	709	78,365.9	2.87	1.269	1	1

Unused: protein identification score; Coverage: confluence ≥95% protein coverage; Spectrum: total spectrum amount; Unique Spectrum: unique spectrum amount. * indicates the potential transcription factor. LPS, lipopolysaccharide.

manner, increasing the exposure of PS to the outside of membrane. This process is crucially involved in many pathophysiologies, such as cell phagocytosis, coagulation, and inflammation (23-25). The research conducted by Wiedmer *et al.* confirmed that the expression levels of PLSCRs in humans and mice are different (6). Furthermore, several studies have examined PLSCR1-3 in the PLSCR family, while considerably less research has focused on the specific effect of PLSCR4 in humans. Our study revealed that when LPS stimulated the HPMECs, the expression of PLSCR4, the concentration of the inflammatory factors, IL-1β and IL-18, and the endothelial permeability all increased. After the silencing of PLSCR4, HPMEC inflammation and permeability were more significantly increased, suggesting that PLSCR4 in endothelial cells have a protective effect.

The next step involved determining the mechanism of the protective effect. Other studies have reported that the expression level of PLSCRs is consistent with the exposure level of PS (26-28).

When the cell is infected, PS is transported outside of the cell membrane by PLSCRs. The increased exposure of the outside of the PS membrane is correlated to various pathophysiological processes, such as apoptosis, pyroptosis, and necroptosis. Studies have revealed that PS is involved in the anchor of the pyroptosis executive protein, GSDMD, in the cell membrane. We thus inferred that PLSCR4 might have an important effect in pyroptosis (29-31), especially

in the early stage of infection (32). Pyroptosis is a newly discovered type of programmed cell death characterized by inflammation after necrosis and apoptosis (14). The main mechanism is that in the presence of noxious stimuli, caspase-1 is activated into its active form, caspase-1 P20 (33). Afterwards, caspase-1 P20 activates the proinflammatory IL-1β and IL-18 to their active forms. Second, caspase-1 P20 cleaves the GSDMD into an active N-terminal fragment, N-GSDMD, which specifically binds to the inner PS (30) of the membrane and forms a homopolymer, a hydrophilic pore in the plasma membrane with a diameter of approximately 10–15 nm, which compromises the integrity of the cell membrane. IL-1β and IL-18 are released to recruit other inflammatory cells, expanding the inflammatory response (34). Hence, pyroptosis is also called inflammatory necrosis of the cell, and can be detected with positive Annxin V-FITC staining. However, PI can stain the cell nucleus through the pores formed by N-GSDMD during pyroptosis and the significant inflammatory response, which does not normally occur in apoptosis. Furthermore, unlike necrosis, the cell morphology usually remains normal in the early stage of pyroptosis (35), and is related to the cellular defense response (36). Recent studies have reported that when stimulated by LPS, pulmonary vascular endothelial cells undergo extensive cell pyroptosis (37-39). Therefore, determining whether PLSCR4 exerts a protective effect on endothelial cells by regulating the distribution of PS has become the main concern of this study. In the results, it was found that when LPS stimulated HPMECs, with the increase in PLSCR4 expression, the Annexin V-FITC staining intensity of PS increased, as did the nucleus staining with PI. When PLSCR4 was silenced, the PS exposure decreased with more GSDMD-NT distribution on the membrane, while the PI staining of the nucleus significantly increased, which is consistent with the change in inflammatory factors in the cell culture medium. This indicated that when the expression of PLSCR4 decreased, the degree of pyroptosis of HPMECs increased. When the experiment used DNA pull-down and protein profiling experiments to further clarify the mechanism of PLSCR4, it was found that PLSCR4 may be regulated by P62280 when stimulated by LPS.

Conclusions

Our study is the first to reveal the protective effect of PLSCR4 and the related mechanism. It was presumed that by transporting PS to the outside of the cell membrane, PLSCR4 could reduce the binding of the pyroptosis executive protein N-GSDMD to PS and the formation of pyroptosis pores, thereby reducing the degree of pyroptosis. Further experiments revealed that the expression of PLSCR4 is mainly regulated by P62280. It is hoped that the experimental results of the present study can provide a new focus for studying endothelial cell damage and new ideas for finding a solution to the clinical treatment of ARDS.

Acknowledgments

We would like to acknowledge the Medical Research Center of Shandong Provincial Qianfoshan Hospital and the Public Technical Service Platform of Shandong University for equipment support.
Funding: This work was supported by the National Natural Science Foundation of China (no.81770076), the Academic promotion program of Shandong First Medical University, and the Distinguished Taishan Scholars and Young Taishan Scholars.

Footnote

Reporting Checklist: The authors have completed the ARRIVE reporting checklist. Available at http://dx.doi.org/10.21037/atm-20-7983

Data Sharing Statement: Available at http://dx.doi.org/10.21037/atm-20-7983

Conflicts of Interest: All authors have completed the ICMJE uniform disclosure form (available at http://dx.doi.org/10.21037/atm-20-7983). The authors have no conflicts of interest to declare.

Ethical Statement: The authors are accountable for all aspects of the work in ensuring that questions related to the accuracy or integrity of any part of the work are appropriately investigated and resolved. Experiments were performed in compliance with the guidelines of Animal Ethics Committee of Qianfoshan Hospital of Shandong University for the care and use of animals. The experiments were approved by the Animal Ethics Committee of Qianfoshan Hospital of Shandong University (No.: 2019-016).

References

1. Akil A, Ziegeler S, Reichelt J, et al. Combined Use of CytoSorb and ECMO in Patients with Severe Pneumogenic Sepsis. Thorac Cardiovasc Surg 2020. [Epub ahead of print]. doi: 10.1055/s-0040-1708479.
2. Auriemma CL, Zhuo H, Delucchi K, et al. Acute respiratory distress syndrome-attributable mortality in critically ill patients with sepsis. Intensive Care Med 2020;46:1222-31.
3. Cheng KT, Xiong S, Ye Z, et al. Caspase-11-mediated endothelial pyroptosis underlies endotoxemia-induced lung injury. J Clin Invest 2017;127:4124-35.
4. Wang D, Gu C, Liu M, et al. Analysis of Long Noncoding RNA Expression Profile in Human Pulmonary Microvascular Endothelial Cells Exposed to Lipopolysaccharide. Cell Physiol Biochem 2019;52:653-67.
5. Wang D, Li Y, Gu C, et al. Identification of Key Pathways and Genes of Acute Respiratory Distress Syndrome Specific Neutrophil Phenotype. Biomed Res Int 2019;2019:9528584.
6. Wiedmer T, Zhou Q, Kwoh DY, et al. Identification of three new members of the phospholipid scramblase gene family. Biochim Biophys Acta 2000;1467:244-53.
7. Bassé F, Stout JG, Sims PJ, et al. Isolation of an erythrocyte membrane protein that mediates Ca2+-dependent transbilayer movement of phospholipid. J Biol Chem 1996;271:17205-10.
8. Gaipl US, Beyer TD, Baumann I, et al. Exposure of anionic phospholipids serves as anti-inflammatory and immunosuppressive signal--implications for antiphospholipid syndrome and systemic lupus erythematosus. Immunobiology 2003;207:73-81.
9. Mulvihill E, Sborgi L, Mari SA, et al. Mechanism of membrane pore formation by human gasdermin-D. EMBO J 2018;37:e98321.
10. Tsuchiya K, Nakajima S, Hosojima S, et al. Caspase-1 initiates apoptosis in the absence of gasdermin D. Nat Commun 2019;10:2091.
11. Chen J, Liu F, Lee SA, et al. Detection of IL-18 and IL-1beta protein and mRNA in human oral epithelial cells induced by Campylobacter concisus strains. Biochem Biophys Res Commun 2019;518:44-9.
12. Bischoff I, Hornburger MC, Mayer BA, et al. Pitfalls in assessing microvascular endothelial barrier function: impedance-based devices versus the classic macromolecular tracer assay. Sci Rep 2016;6:23671.
13. He WT, Wan H, Hu L, et al. Gasdermin D is an executor of pyroptosis and required for interleukin-1beta secretion. Cell Res 2015;25:1285-98.
14. Fink SL, Cookson BT. Apoptosis, pyroptosis, and necrosis: mechanistic description of dead and dying eukaryotic cells. Infect Immun 2005;73:1907-16.
15. He Y, Hara H, Nunez G. Mechanism and Regulation of NLRP3 Inflammasome Activation. Trends Biochem Sci 2016;41:1012-21.
16. Lamkanfi M, Dixit Vishva M. Mechanisms and Functions of Inflammasomes. Cell 2014;157:1013-22.
17. Bergsbaken T, Fink SL, Cookson BT. Pyroptosis: host cell death and inflammation. Nat Rev Microbiol 2009;7:99-109.
18. Chen X, He WT, Hu L, et al. Pyroptosis is driven by non-selective gasdermin-D pore and its morphology is different from MLKL channel-mediated necroptosis. Cell Res 2016;26:1007-20.
19. Angus DC, van der Poll T. Severe sepsis and septic shock. N Engl J Med 2013;369:840-51.
20. Bhattacharya J, Matthay MA. Regulation and repair of the alveolar-capillary barrier in acute lung injury. Annu Rev Physiol 2013;75:593-615.
21. Wang L, Liu J, Xie W, et al. Overexpression of MALAT1 Relates to Lung Injury through Sponging miR-425 and Promoting Cell Apoptosis during ARDS. Can Respir J 2019;2019:1871394.
22. Chambers E, Rounds S, Lu Q. Pulmonary Endothelial Cell Apoptosis in Emphysema and Acute Lung Injury. Adv Anat Embryol Cell Biol 2018;228:63-86.
23. Bevers EM, Comfurius P, Zwaal RF. Platelet procoagulant activity: physiological significance and mechanisms of exposure. Blood Rev 1991;5:146-54.
24. Fadok VA, Voelker DR, Campbell PA, et al. Exposure of phosphatidylserine on the surface of apoptotic lymphocytes triggers specific recognition and removal by macrophages. J Immunol 1992;148:2207-16.
25. Verhoven B, Schlegel RA, Williamson P. Mechanisms of phosphatidylserine exposure, a phagocyte recognition signal, on apoptotic T lymphocytes. J Exp Med 1995;182:1597-601.
26. Wolfs JL, Comfurius P, Rasmussen JT, et al. Activated

scramblase and inhibited aminophospholipid translocase cause phosphatidylserine exposure in a distinct platelet fraction. Cell Mol Life Sci 2005;62:1514-25.
27. Lang PA, Kempe DS, Akel A, et al. Inhibition of erythrocyte "apoptosis" by catecholamines. Naunyn Schmiedebergs Arch Pharmacol 2005;372:228-35.
28. Zwaal RF, Comfurius P, Bevers EM. Scott syndrome, a bleeding disorder caused by defective scrambling of membrane phospholipids. Biochim Biophys Acta 2004;1636:119-28.
29. Ding J, Wang K, Liu W, et al. Pore-forming activity and structural autoinhibition of the gasdermin family. Nature 2016;535:111-6.
30. Liu X, Zhang Z, Ruan J, et al. Inflammasome-activated gasdermin D causes pyroptosis by forming membrane pores. Nature 2016;535:153-8.
31. Martinon F, Burns K, Tschopp J. The inflammasome: a molecular platform triggering activation of inflammatory caspases and processing of proIL-beta. Mol Cell 2002;10:417-26.
32. Galle JN, Hegemann JH. Exofacial phospholipids at the plasma membrane: ill-defined targets for early infection processes. Biol Chem 2019;400:1323-34.
33. Feria MG, Taborda NA, Hernandez JC, et al. HIV replication is associated to inflammasomes activation, IL-1β, IL-18 and caspase-1 expression in GALT and peripheral blood. PLoS One 2018;13:e0192845.
34. Schneider KS, Groß CJ, Dreier RF, et al. The Inflammasome Drives GSDMD-Independent Secondary Pyroptosis and IL-1 Release in the Absence of Caspase-1 Protease Activity. Cell Rep 2017;21:3846-59.
35. Vande Walle L, Lamkanfi M. Pyroptosis. Curr Biol 2016;26:R568-72.
36. de Vasconcelos NM, Lamkanfi M. Recent Insights on Inflammasomes, Gasdermin Pores, and Pyroptosis. Cold Spring Harb Perspect Biol 2020;12:a036392.
37. He X, Qian Y, Li Z, et al. TLR4-Upregulated IL-1β and IL-1RI Promote Alveolar Macrophage Pyroptosis and Lung Inflammation through an Autocrine Mechanism. Sci Rep 2016;6:31663.
38. Wu D, Pan P, Su X, et al. Interferon Regulatory Factor-1 Mediates Alveolar Macrophage Pyroptosis During LPS-Induced Acute Lung Injury in Mice. Shock 2016;46:329-38.
39. Yang J, Zhao Y, Zhang P, et al. Hemorrhagic shock primes for lung vascular endothelial cell pyroptosis: role in pulmonary inflammation following LPS. Cell Death Dis 2016;7:e2363.

(English Language Editor: J. Gray)

Cite this article as: Liu X, Wang D, Zhang X, Lv M, Liu G, Gu C, Yang F, Wang Y. Effect and mechanism of phospholipid scramblase 4 (PLSCR4) on lipopolysaccharide (LPS)-induced injury to human pulmonary microvascular endothelial cells. Ann Transl Med 2021;9(2):159. doi: 10.21037/atm-20-7983

